Skin carcinogenesis in mice using UVB radiation

Nguyen Phuong Khanh[1*], Nguyen Hoang Tan[1], Le Thi Hoang Uyen[1], Le Thi Hong Ngan[1]

[1]International University - Vietnam National University - HCMC, Vietnam
[*]Corresponding author: phuongkhanh.nguyen511@gmail.com

ARTICLE INFO

DOI:10.46223/HCMCOUJS.tech.en.12.1.1880.2022

Received: May 17th, 2021

Revised: June 27th, 2021

Accepted: July 22nd, 2021

Keywords:

mice skin cancer; non-melanoma skin cancer; squamous cell skin sarcinoma; UVB-radiated

ABSTRACT

Ultraviolet B (UVB) radiation is directly related to sunburn and other visible changes on the skin surface, including discoloration and skin carcinoma. This study investigates the influence of UVB rays (wavelength from 290 - 320nm) on the formation of cancerous tissues and also shows the differences between abnormal and normal tissue. The mice were stimulated with DMBA chemical protocol and exposed to UVB radiation for skin carcinogenesis. Normal and cancerous skin tissue were stained with Hematoxylin and Eosin, they were measured to obtain optical properties by applying Mueller-Matrix Decomposition, which is considered an effective skin structure analysis method. Long-term exposure to UVB radiation caused skin inflammation and the appearance of crystal bumps. Histopathology results clearly indicate the increasing number of papilloma cells and prolonged damage by UVB radiation. Skin structural analysis was specified with the optical parameters by the Mueller Matrix Decomposition method. The extension of skin carcinoma significantly lessened the values of Linear Birefringence (LB) and Circular Birefringence (CB), as well as the variation of Linear Dichroism (LD) and Circular Dichroism (CD) parameters help validate the differences between normal and squamous cell skin sample.

1. Introduction

The skin is the largest organ in the human body; it holds an important role in keeping balance homeostasis and protecting the human body from ultraviolet radiation (UVR). Imbalance homeostasis, UVR attack can lead to RNA damage, pigmentary changes, effect on skin-eyes-immunity health, even life-threatening carcinoma (Ichihashi et al., 2003). Nowadays, increasing rates of skin cancer are likely due to a UVR combination exposure, when people perform outdoor activities, the break-in fashion design, or due to lifespan elongation, genetic regulation, or potentially ozone destruction (Le, Huynh, Nguyen, Vo, & Pham, 2018). The statistics of WHO (World Health Organization, n.d.), which is up to nearly 3 million non-melanoma and hundred thousand melanoma skin carcinoma cases worldwide annually (Wilson, Moon, & Armstrong, 2012).

Skin cancer apparently includes two types: non-melanoma and melanoma skin cancers. In the first type, non-melanoma, the combination of Squamous Cell Carcinomas (SCCs) and Basal Cell Carcinomas (BCCs), is the most common type of human skin cancer. UVR further includes various sub-types: UVA (320 - 400nm), UVB (280 - 320nm), and UVC (200 - 280nm), respectively (Wilson et al., 2012). UVA rays penetrate deeper into the skin through both the epidermis and dermis. However, it is considered not to be a strong carcinogenic factor. UVC has

the shortest wavelength and is defined to be the most dangerous; however, it is mostly blocked by the ozone layer. Our skin and eyes mostly take up the wavelengths of UVB in the portion of the solar spectrum, which easily leads to erythema, burns, and sooner or later skin carcinoma. Therefore, targeting signal molecules induced by UVB is one of the effective techniques to prevent skin tumorigenesis.

Many studies experimented with skin carcinoma models by using UVB lamps with peak emission ranges approximately 290 - 310nm and performed in a UVB chamber, the radiated time lasting from 16 to 20 weeks. After 23 weeks, the average number of tumors per mouse was 07 in the hairless fat-1 mice compared with 16.5 in the WT hairless mice (UVB-radiated group) (Yum et al., 2017). In Zhang et al. (2005) study, development and proliferation of p53 mutant clones, precancer formation, and malignant conversion of precancers to carcinoma in situ and SCC are among the carcinogenic events caused by UVB radiation. Thus, UVB is one of the critical elements in the development of UVB-induced skin tumors as well as oxidative stress and inflammation in the skin.

The most frequent polycyclic aromatic hydrocarbon utilized as a starting agent in chemically induced skin cancer models is 7,12-dimethylbenz(a)anthracene (DMBA). By creating covalent adducts with the DNA of epidermal cells and primary keratinocyte stem cells, DMBA causes random DNA mutations. Some of these random mutations occur in proto-oncogenes like Hras1 (mutations in Kras and Nras have also been identified), and the conversion of proto-oncogenes to oncogenes promotes tumor development when the right stimuli are applied. Therefore, DMBA is a potentially proto-cancer agent to stimulate skin cells to become more sensitive to the effects of UVB. The combination of 0.2% DMBA solution and 2% croton oil solution was implemented in the research of Le et al. (2018) with a period of two times per week for a total of 20 weeks and showed the distinct structure of cancerous and normal mice skin.

Stoke parameters and Mueller matrix method is crucial for determining the optical characteristics of optoelectronic and biological materials. A decoupled analytical strategy based on the Mueller matrix method and the Stokes parameters is proposed on deriving effective parameters of anisotropic optical materials in Linear Birefringence (LB), Linear Dichroism (LD), Circular Birefringence (CB), and Circular Dichroism (CD) characteristics (Pham & Lo, 2012a). Moreover, Linear Dichroism (LD) measurements of human tissue can facilitate tumor determination, whereas Circular Dichroism (CD) measurements are a successful means of characterizing and classifying protein structures. CD examinations give a reliable implication of classifying distinctive proteins (Pham & Lo, 2012b). In expansion, CD spectroscopy is additionally broadly utilized to test a wide range of optically active (chiral) materials, extending from small molecules to macromolecules (Pham & Lo, 2012a).

In this study, we applied DMBA for the first stage of skin carcinogenesis and then performed UVB radiation on the UVB-radiated group for the promotion stage in 12 weeks, with a UVB rate of 0.257J/cm^2 each. The comparison between the UVB-radiated and normal skin tissues was implemented by the Stoke-Muller matrix decomposition methodology with effective optical parameters: Linear Birefringence (LB), Linear Dichroism (LD), Circular Birefringence (CB), Circular Dichroism (CD), Linear Depolarization (L-Dep) and also Circular Depolarization (C-Dep) properties.

2. Materials and methods

2.1. UVB radiation-induced skin carcinogenesis study

In our study, we apply a UVB radiation lamp (Philips TL20W/01 RS) that emits wavelengths from 280 to 320nm, peaking at 311nm. The lamp radiation rate is measured at

0.257J/cm^2 on average 13 minutes, by Ophir UV-radiometer.

The experiment was conducted on 15 healthy Swiss male mice (20 to 35g)purchased from the Pasteur Institution of Nha Trang (IVAC, Vietnam). The animals were divided into two groups: the normal group (three mice) and UVB radiated group (12 mice). The mice were kept individually locked to each cage to ensure adaptation. Mice were maintained at 12/12h light/dark cycle within three days, freely using food pellets and water during the experiment. The back skin of mice was shaved for an 2cm x 3cm area before applying carcinogenesis chemical protocol.

Twelve experimented mice were irradiated three times weekly at the dose of 0.257J/cm^2 each, unrestrained from above with thin steel mesh covers (Figure 1A). The UVB lamp (305-315nm, peak at 311nm) (Philips TL20W/01 RS) was installed into a private wooden chamber and covered with black fabric (Figure 1B), avoiding the UVB-irradiated to the surrounding area. The distance between the mice cage and the UVB lamp was measured at about 15cm.

Figure 1. Mice skin carcinogenesis model. Mice irradiated box (A), UVB wooden chamber (B)

2.2. Mice skin carcinogenesis chemical protocol

All chemicals were bought from Sigma-Aldrich Co, consisting of 7,12-Dimethylbenz[a]anthracene (≥ 95%) (DMBA), Hematoxylin, and Eosin stain.

50uL DMBA solution (0.2% prepared in acetone) was applied to the shaved dorsal skin only once at the initial stage of the experiment (each mouse was equivalently received 100µg DMBA). After two days, UVB exposure was applied to the group of radiated mice, with a dose of three times every week to irritate the skin carcinoma pathology. In the 15th week, skin tissues were collected then processed for optical parameters purposes. The specimens, which were sliced thinly to a thickness of 05µm, were contained on the Quartz slides to ensure absolute disinfection. The slides were then analyzed and compared using the optical polarimetry system, which is the Stokes-Mueller matrix decomposition method.

Cancerous biological tissues which had 05µm thickness were manually segmented and marked with Hematoxylin and Eosin stain. The integration between two histological stains has occurred during H&E. The hematoxylin stains cell nuclei blue, and eosin stains the extracellular matrix and cytoplasm pink (Tsai et al., 2012). Consequently, other structures will illustrate in different shades, special colors, and combinations of these colors. The H&E procedure can be used to diagnose a host of histopathologic conditions which consists of cancer. To conclude, this study is a helpful technique for cancer detection because it provides a precise view of tissue by clearly staining cell structures and identifying distinctions between organelles. Finally, the stained slides were perused beneath a light microscope for analyzing histopathology.

2.3. Mueller matrix decomposition method for effective parameters extraction

Depending on Pham and Lo's analytical technique (Pham & Lo, 2012a), named decomposition of the Mueller matrix and polarimetry of the Stokes vector, the experiment based on four separate input polarization lights to extract the effective measurements: the LB orientation angle (α), phase retardance (β), optical rotation angle (γ), LD orientation angle (θd), linear dichroism (D), circular dichroism (R), linear depolarization (e1, e2), and circular depolarization (e3) of normal and skin cancer samples. Originally, this technique was used to extract the optical parameters of anisotropic materials by Pham and Lo (2012a). Later, many scientists applied this method to the optical characterization of biological samples such as human blood plasma, collagen solution, and calfskin. Furthermore, this method is considered to have potential in skin structural analysis, noninvasive diagnosis in glucose, and collagen measurements.

The formula of output Stokes vector, S can be expressed where $\hat{S}_c$is input Stokes vectors:

$$S_c = \begin{bmatrix} S_0 \\ S_1 \\ S_2 \\ S_3 \end{bmatrix}_C = M_\Delta M_{lb} M_{cb} M_{ld} M_{cd} \hat{S}_c = \begin{pmatrix} m_{11} & m_{12} & m_{13} & m_{14} \\ m_{21} & m_{22} & m_{23} & m_{24} \\ m_{31} & m_{32} & m_{33} & m_{34} \\ m_{41} & m_{42} & m_{43} & m_{44} \end{pmatrix} \begin{pmatrix} \hat{S}_0 \\ \hat{S}_1 \\ \hat{S}_2 \\ \hat{S}_3 \end{pmatrix}_c \quad (1)$$

and M_Δ, M_{lb}, M_{cb},M_{ld},M_{cd} are the Muller matrices of depolarization index and effective LB, CB, LD, CD parameters of sample, respectively. Accordingly, the value must be non-zero from element m_{11} to m in Equation (1). In the setup of Figure 2, the input lights of four linear polarization (i.e., $\hat{S}_{0^\circ} = [1,1,0,0]^{\mathrm{T}}$, $\hat{S}_{45^\circ} = [1,0,1,0]^{\mathrm{T}}$, $\hat{S}_{90^\circ} = [1,-1,0,0]^{\mathrm{T}}$ and $\hat{S}_{135^\circ} = [1,0,-1,0]^{T}$) and two circular polarization (i.e., right-handed $\hat{S}_{\mathrm{RHC}^\circ} = [1,0,0,1]^{\mathrm{T}}$ and left-handed $\hat{S}_{\mathrm{LHC}^\circ} = [1,0,0,-1]^{\mathrm{T}}$).

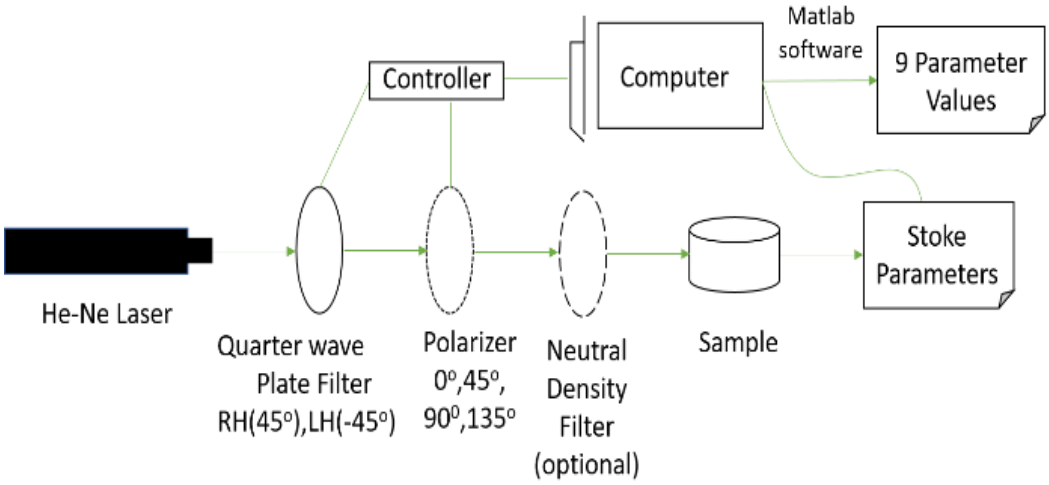

Figure 2. Schematic illustration of Stokes-Mueller Matrix

The system includes He-Ne laser (HNLS008R, Thorlabs Co.), quarter-wave plate filter (QWP0-63304-4-R10, CVI Co.), polarizer (GTH5M, Thorlabs, Co.), neutral density filter (NDC-100-2, ONSET Co.), and Stokes polarimeter (PAX5710, Thorlabs Co.).

First, the He-Ne laser produced a light with a central wavelength of 633nm. Secondly, the quarter-wave plate filter received He-Ne laser input light and filtered into left/right circular polarization lights. For the linear orientation, the polarizer would be categorized into different linear polarization lights (0deg, 45deg, 90deg, 135deg). A neutral density filter was put in the

middle to maintain the intensities of every input polarization light. Finally, the results were obtained and computed by using a Stokes polarimeter. The samples were fixed steadily to a side stand between the polarizer and the detector.

3. Results

3.1. UVB exposure cause skin inflammation

The result of DMBA stimulation combined with UVB-radiation on mice skin areas was examined and compared to control groups. At the 4th week of the experiment, the expected mice skin areas lost moisture, became drier, and started flaking (Figure 3A). In this stage, the epidermis layer is affected, causing skin inflammation, which is one of the common signs of precancer. The status of mice was noted to be uneasy, often bite their experimented skin area, and reacted uncomfortably to executors. Figure 3B illustrates the status after eight weeks of experiments; the mice skin area started appearing red and small crystal bumps. In this stage, the dermis-inner layer of the skin is affected; also, inflammation spreads out to surrounding areas. From the 12th week of the experiment, the surrounding areas started to appear with small crystal bumps (Figure 3C).

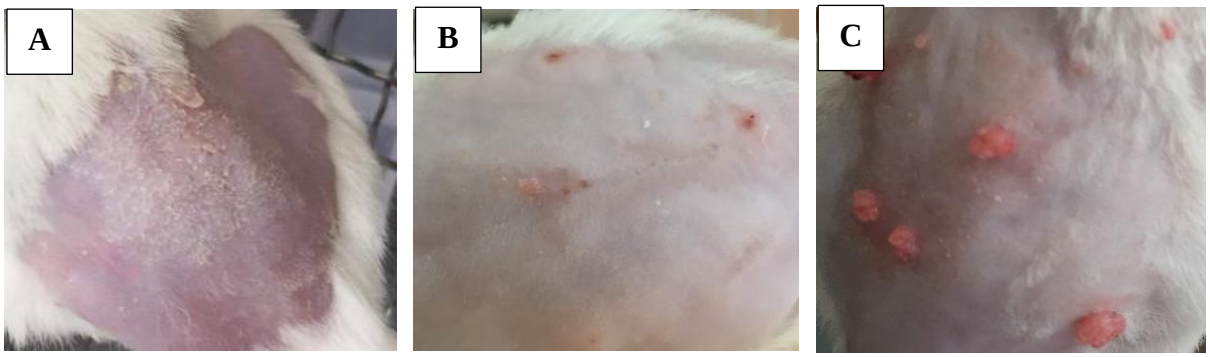

Figure 3. Effect of UVB-radiated on mice. Mice skin after one month (A), Mice Skin after two months (B), Mice skin after three months (C)

3.2. Histopathological analysis

Figure 4 shows the histopathological morphology of two representative groups of samples. Figure 4A demonstrated the control group, while Figures 4B and 4C revealed the UVB radiated group. Figure 4B with the yellow arrow illustrates an increase of papilloma cells. Meanwhile, Figure 4C showed not only the UV damage to the skin by prolonged UVB radiation but also a wide range of inflammatory skin cells that were indicated by a red arrow. The histopathological results showed part of the evidence for the increase of squamous cell carcinoma as well as the papilloma cells in the radiated mice samples.

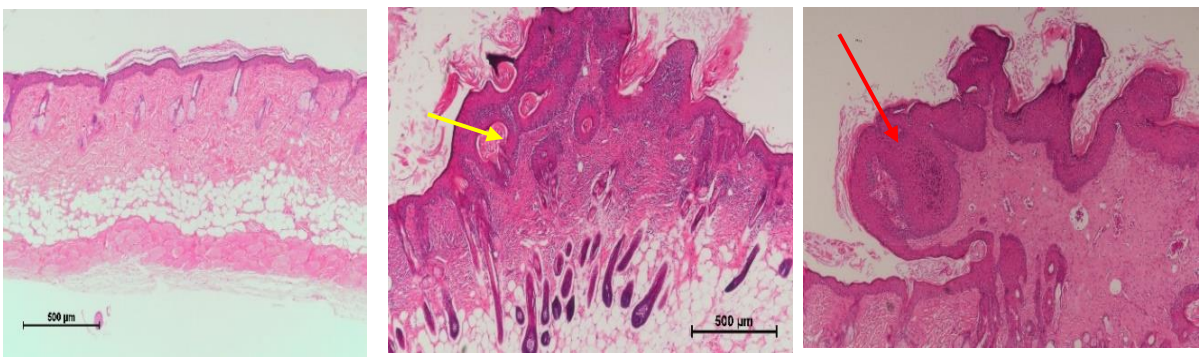

Figure 4. The results of histopathology of subjects. Control group (A), UVB-Radiated group (B), (C)

3.3. Optical properties of non-melanoma tumors

Figure 5 shows nine effective properties of squamous mice skin carcinoma. Overall, all of the optical properties obtained from six subjects reveal similarities. However, there are differences in the orientation angle of CB (γ_S) and CD circular dichroism (R_S). Specifically, in Figure 5(A), orientation angles of LB (β_S) are reaching 140 - 160deg; meanwhile, the variation of LB (α_S) remains stable, approximately 0.5deg. Besides, Figure 5(B) highlights data on CB properties leveled off with three first subjects then increased to 94deg in the subject four and decreased to 90deg at the end. Regarding Figure 5(C), the majority of linear dichroism (θ_S) parameters fluctuate to nearly 0.7. Additionally, there was a substantial variation by CD properties, reaching a peak at 0.37 in the beginning before fluctuating from 0.33 to 0.35 over the subjects shown in Figure 5(D). The depolarization index, which is shown in Figure 5(E), shifts slightly from 0.15 - 0.25. Figure 5(F) indicates that the linear depolarization (e_{1S}, e_{2S}, and e_{3s}) and circular depolarization are approximately 0.98, 0.95, and 1, respectively.

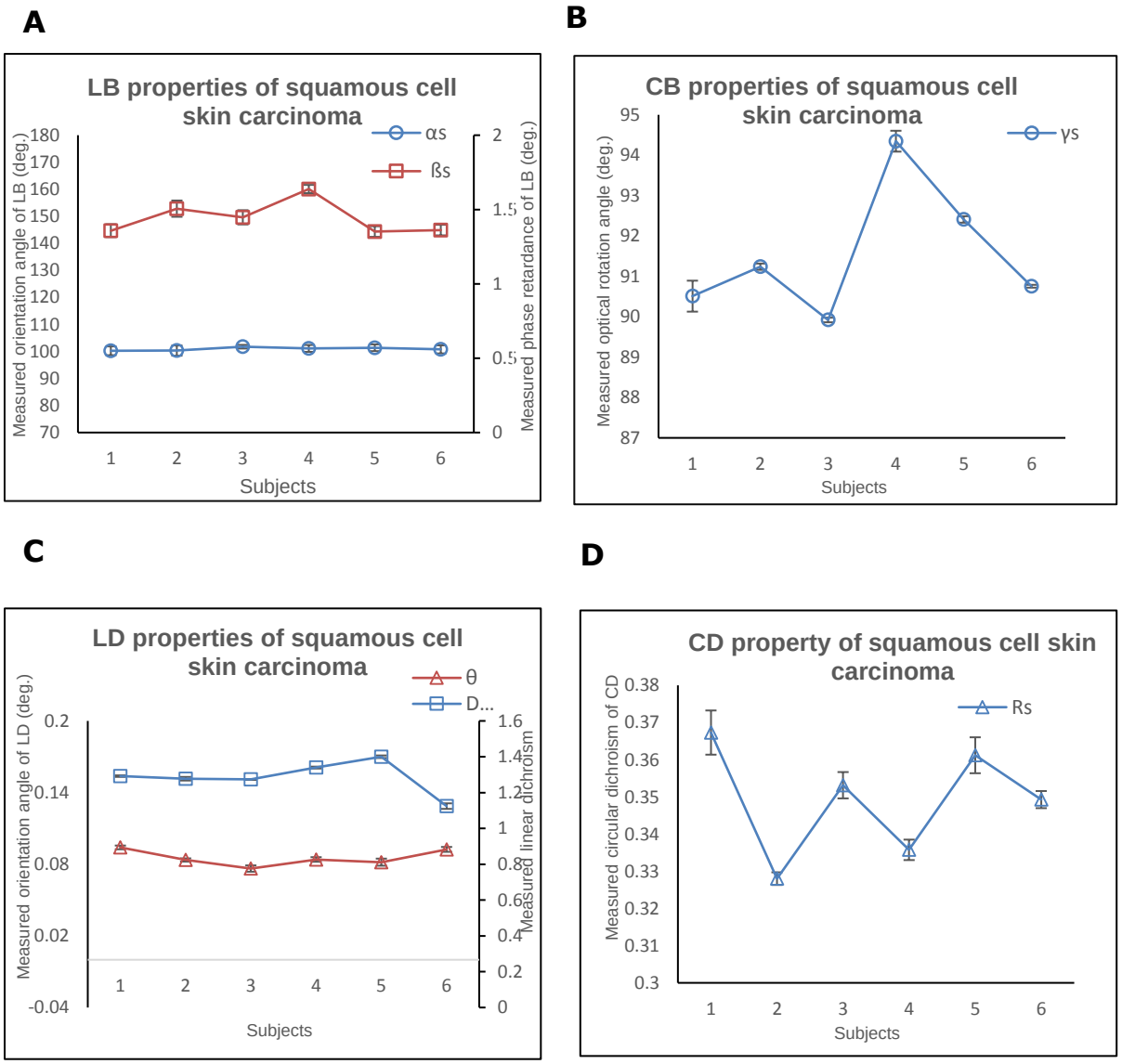

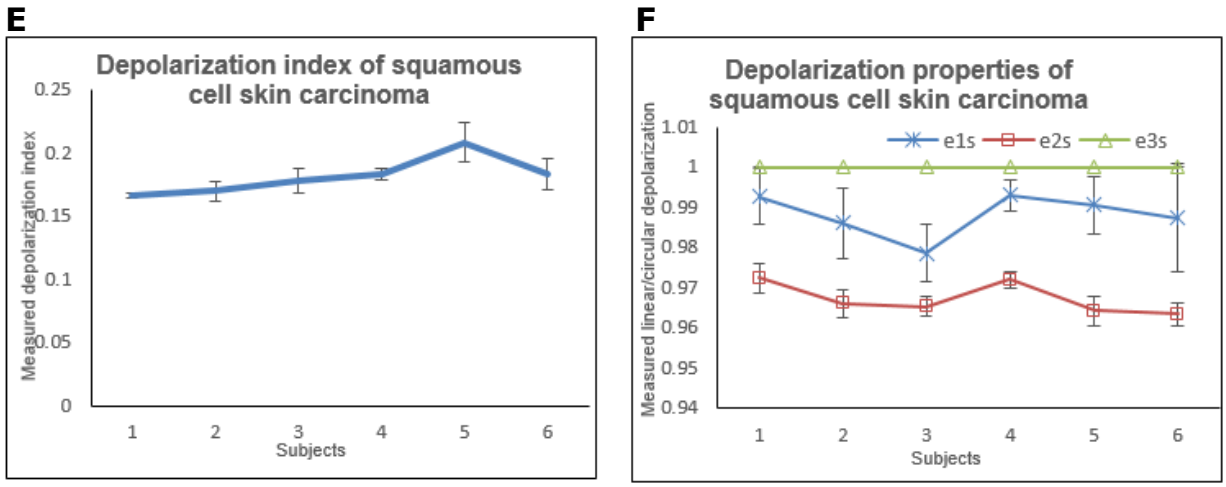

Figure 5. Optical characteristics of (A) orientation angles of LB (α_S) and LB (β_S); (B) optical rotation of CB (γ_S); (C) orientation angle of LD (θ_S) and linear dichroism (D_S); (D) circular dichroism (R_S); (E) depolarization index of squamous cell skin carcinoma on mice; (F) linear depolarization (e_{1S}, e_{2S}, and e_{3S})

Table 1 illustrates measured parameters by the Stokes-Mueller technique. A wide range of those numbers was compared between normal and squamous cell skin carcinoma subjects. The parameters were calculated based on the average, the standard deviation which was taken from six measuring points of 40 specimens obtained from 12 non-melanoma carcinoma subjects. In addition, 15 specimens obtained from three normal subjects were also calculated as demonstrated.

Table 1

Optical parameters of normal and squamous cell skin carcinoma on mice

		α	β	γ	θd	D	R	e_1	e_2	e_3	Δ
Normal	Mean	159.52	44.34	91.51	0.57	1.98	0.35	0.98	-0.98	1	0.83
	SD	0.56	1.18	1.65	0.05	0.15	0.02	0.01	0.01	0	0.05
Squamous Cell Skin Carcinoma	Mean	100.10	2.45	146.61	0.09	1.29	0.03	0.99	0.96	1	0.18
	SD	1.56	0.12	2.26	0.01	0.09	0.02	0.01	0.00	0	0.02

Source: Data analysis result of the research

LB properties (Figure 6A, 6B) of the UVB radiated group recorded significantly lower than the normal group. The estimates of alpha and beta of the normal group are around 159.87deg and 34.45deg, while those in the radiated group are approximately 97.34deg and 1.39deg, respectively. Although smaller fluctuations compared to LB properties, CB properties (Figure 6C) have noticeable variations. The Δ measurement of the radiated group is around 158deg, approximately 1.8 times the normal group Δ measurement, 90deg. Meanwhile, the measurement of LD properties (Figure 6D) of the normal group and the radiated group oscillates nearly 1.95deg and 1.3deg, obviously. The depolarization value of the normal group is around 0.18, whereas the radiated group is approximately 0.9, as shown in Figure 7. The distinct depolarization of normal and radiated groups illustrated the broad error bar occurring in many subjects, determining that the measurements calculated are relatively distributed. As a whole, considerable differences between normal and radiated mice groups were identified by the five parameters above.

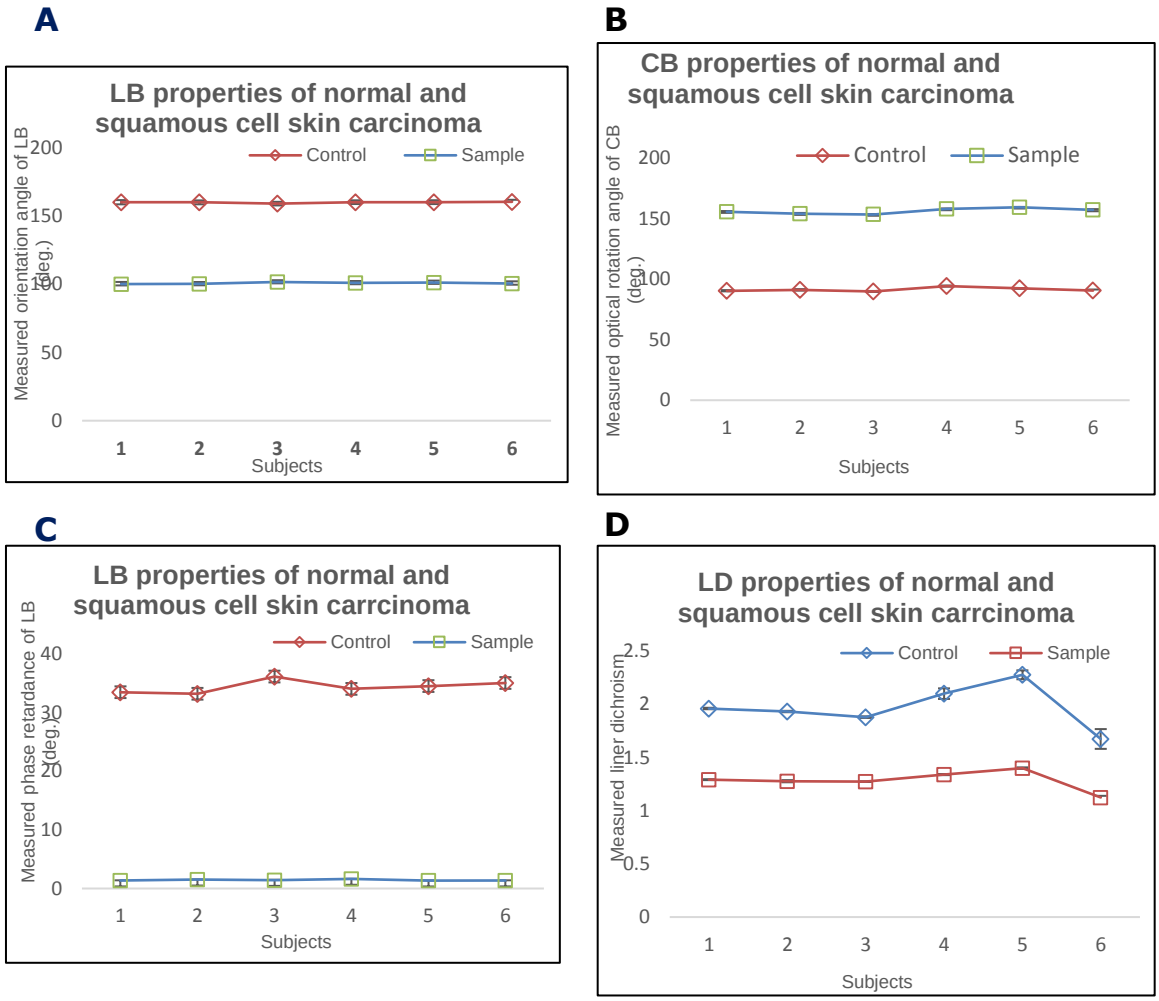

Figure 6. Optical properties comparison of normal and squamous cell skin carcinoma on mice. (A) orientation angles of LB (α_S). (B) CB properties. (C) phase retardations of LB (β_S). (D) LD properties

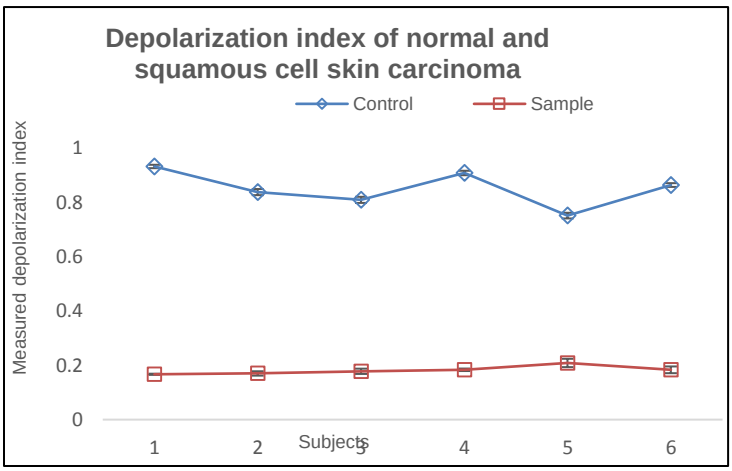

Figure 7. Depolarization index of normal and squamous cell skin carcinoma on mice

4. Discussion

The properties extracted from the Stokes-Mueller matrix decomposition method include effective LB, CB, LD, CD, and depolarization parameters, which helps validate the differences between normal and squamous cell skin samples.

Each LB, CB, LD measurement in the radiated group, including LB alpha 97.34deg, LB beta 1.9deg, CB 158deg, and LD 1.3deg, indicated the distinct values which compared to the normal group, LB alpha 165deg, LB beta 34deg, CB 95deg, and LD 1.8deg, respectively. The significant difference of measured parameters between the two groups is evidence for the presence of cancer cells.

DMBA initiator and UVB radiation are crucial factors for creating squamous cell carcinoma in mice (Le et al., 2018; Phillips et al., 2013); the tumors were presented after 24 weeks with the initial stage for ten consecutive days and the promotion stage three times per week. In our study, we used DMBA for the initial stage of skin carcinogenesis and then applied it three times/week in 20 minutes for the promotion stage, with the UVB rate of 0.257J/cm^2. The results showed that UVB radiated areas were inflamed, and tumors appeared at the 12th week. Therefore, the combination of DMBA and UVB radiation was used to reduce UVB radiation time and increase the status of skin cancer.

5. Conclusion

Our studyfound that the skin carcinoma process with the combination of DMBA and UVB radiation was better than the single UVB methodology. The measured parameters include LB, CB, LD, CD, and depolarization indicated differences between normal and UVB-induced mice skin tissue. Skin carcinoma models are useful in many research applications as in optics and medicine aspects, which helps validate the effect of appropriate treatment procedures.

ACKNOWLEDGEMENTS

This study is funded by International University, Vietnam National University HCMC (VNU-HCM) under grant number SV2019-BME-04.

References

Burns, E. M., Tober, K. L., Riggenbach, J. A., Kusewitt, D. F., Young, G. S., & Oberyszyn, T. M. (2013). Extended UVB exposures alter tumorigenesis and treatment efficacy in a murine model of cutaneous squamous cell carcinoma. *Journal of Skin Cancer, 2013*, Article 246848. doi:10.1155/2013/246848

Guillermo, R. F., Zhang, X., Kaushik, R. S., Zeman, D., Ahmed, S. A., Khalifa, S., … Dwivedi, C. (2012). Dose-response on the chemopreventive effects of sarcophine-diol on UVB-induced skin tumor development in SKH-1 hairless mice. *Marine Drugs, 10*(9), 2111-2125. doi:10.3390/md10092111

Huynh, T. N., Nguyen, D. T., Vo, T. V., & Pham, T. T. (2018). Characterization of healthy and nonmelanoma-induced mouse utilizing the Stokes-Mueller decomposition. *Journal of Biomedical Optics, 23*(12), 1-8.

Ichihashi, M., Ueda, M., Budiyanto, A., Bito, T., Oka, M., Fukunaga, M., … Horikawa, T. (2003). UV-induced skin damage. *Toxicology, 189*(1/2), 21-39.

Jung, S. K., Lee, K. W., Byun, S., Kang, N. J., Lim, S. H., Heo, Y. S., … Dong, Z. (2008). Myricetin suppresses UVB-induced skin cancer by targeting Fyn. *Cancer Research, 68*(14), 6021-6029.

Kremer, J. L., Melo, G. P., Marinello, P. C., Bordini, H. P., Rossaneis, A. C., Sábio, L. R., … Luiz, R. C. (2019). Citral prevents UVB-induced skin carcinogenesis in hairless mice. *Journal of Photochemistry*

and Photobiology B: Biology, 198, Article 111565. doi:10.1016/j.jphotobiol.2019.111565

Le, D. L., Huynh, T. N., Nguyen, D. T., Vo, T. V., & Pham, T. T. (2018). Characterization of healthy and nonmelanoma-induced mouse utilizing the Stokes-Mueller decomposition. *Journal of Biomedical Optics*, *23*(12), 1-8.

Leiter, U., Eigentler, T., & Garbe, C. (2014). Epidemiology of skin cancer. *Advances in Experimental Medicine and Biology, 810*, 120-140.

Matsumura, Y., & Ananthaswamy, H. N. (2004). Toxic effects of ultraviolet radiation on the skin. *Toxicology and Applied Pharmacology, 195*(3), 298-308.

Pham, T. T., & Lo, Y. L. (2012a). Extraction of effective parameters of anisotropic optical materials using a decoupled analytical method. *Journal of Biomedical Optics, 17*(2), Article 025006.

Pham, T. T., & Lo, Y. L. (2012b). Extraction of effective parameters of turbid media utilizing the Mueller matrix approach: Study of glucose sensing. *Journal of Biomedical Optics, 17*(9), Article 097002.

Phillips, J., Moore-Medlin, T., Sonavane, K., Ekshyyan, O., McLarty, J., & Nathan, C. A. (2013). Curcumin inhibits UV radiation-induced skin cancer in SKH-1 mice. *Otolaryngology-head and neck surgery: Official journal of American Academy of Otolaryngology-Head and Neck Surgery, 148*(5), 797-803.

Tsai, K. D., Lin, J. C., Yang, S. M., Tseng, M. J., Hsu, J. D., Lee, Y. J., & Cherng, J. M. (2012). Curcumin protects against UVB-induced skin cancers in SKH-1 hairless mouse: Analysis of early molecular markers in carcinogenesis. *Evidence-based Complementary and Alternative Medicine*, *2012*(6), Article 593952.

Wilson, B. D., Moon, S., & Armstrong, F. (2012). Comprehensive review of ultraviolet radiation and the current status on sunscreens. *The Journal of Clinical and Aesthetic Dermatology, 5*(9), 18-23.

Wood, M. F., Ghosh, N., Moriyama, E. H., Wilson, B. C., & Vitkin, I. A. (2009). Proof-of-principle demonstration of a Mueller matrix decomposition method for polarized light tissue characterization in vivo. *Journal of Biomedical Optics, 14*(1), Article 014029.

World Health Organization. (n.d.). *Radiation: Ultraviolet (UV) radiation and skin cancer*. Retrieved January 10, 2021, from World Health Organization website: https://www.who.int/news-room/q-a-detail/radiation-ultraviolet-(uv)-radiation-and-skin-cancer.

Yum, H. W., Park, J., Park, H. J., Shin, J. W., Cho, Y. Y., Kim, S. J., … Surh, Y. J. (2017). Endogenous ω-3 fatty acid production by FAT-1 transgene and topically applied docosahexaenoic acid protect against UVB-induced mouse skin carcinogenesis. *Scientific Reports, 7*(1), Article 11658.

Zhang, W., Hanks, A. N., Boucher, K., Florell, S. R., Allen, S. M., Alexander, A., … Grossman, D. (2005). UVB-induced apoptosis drives clonal expansion during skin tumor development. *Carcinogenesis*, *26*(1), 249-257.